

M 62 56317

NACA TN 4317

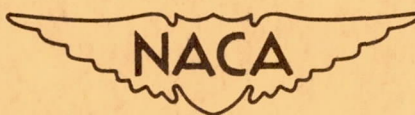
# NATIONAL ADVISORY COMMITTEE FOR AERONAUTICS

TECHNICAL NOTE 4317

TURBOJET ENGINE NOISE REDUCTION WITH MIXING  
NOZZLE-EJECTOR COMBINATIONS

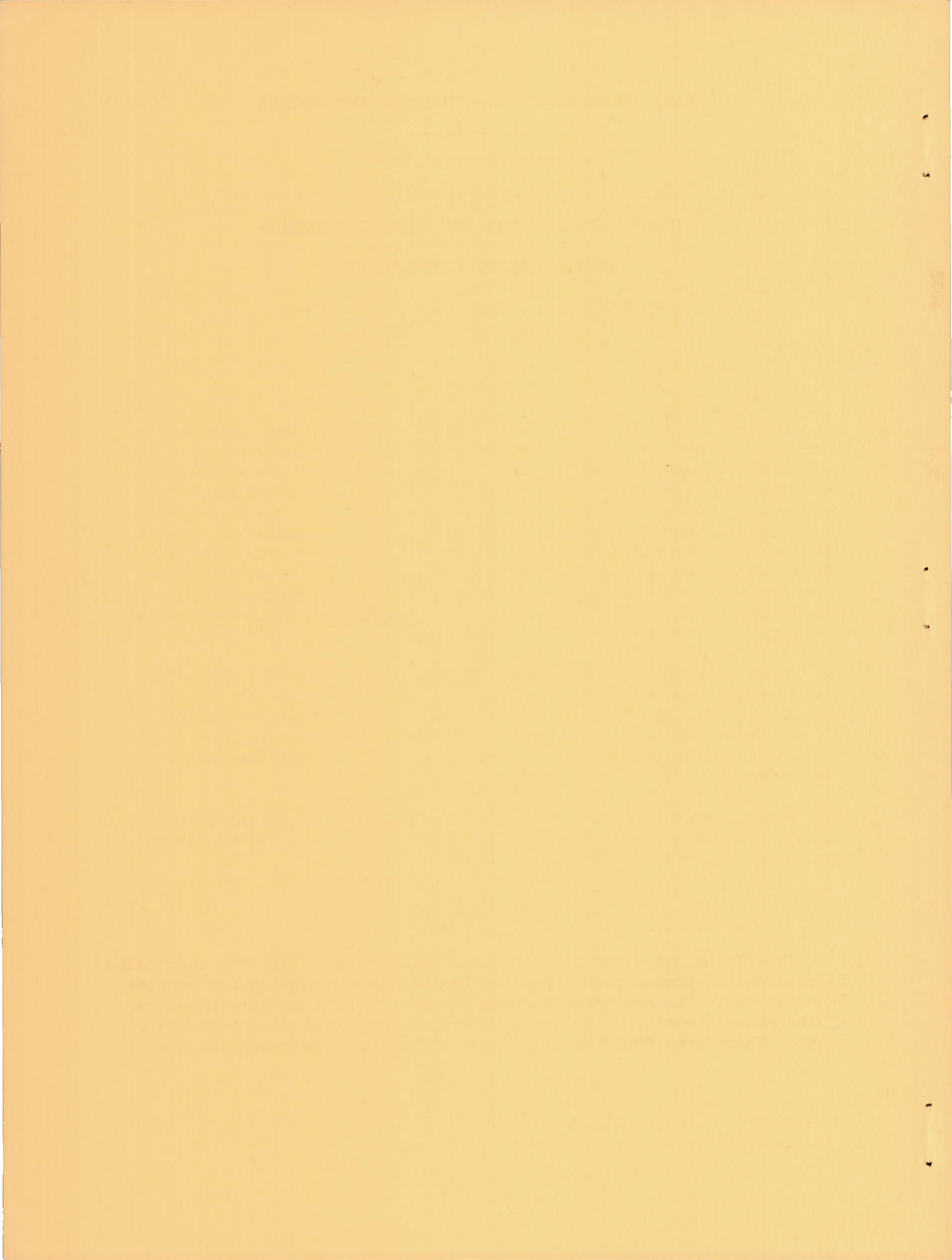
By Willard D. Coles, John A. Mihalow and Edmund E. Callaghan

Lewis Flight Propulsion Laboratory  
Cleveland, Ohio



Washington

August 1958



NATIONAL ADVISORY COMMITTEE FOR AERONAUTICS

TECHNICAL NOTE 4317

TURBOJET ENGINE NOISE REDUCTION WITH MIXING

NOZZLE-EJECTOR COMBINATIONS

By Willard D. Coles, John A. Mihalow  
and Edmund E. Callaghan

SUMMARY

Several noise suppressors consisting of combinations of mixing nozzles and ejectors were tested on two full-scale turbojet engines. Maximum sound pressure level reductions of 12 decibels and sound power level reductions of 8 decibels were obtained. The ejectors provided 3 to 5 decibels of the sound power reduction. The effects of ejector dimensions on noise suppression and engine performance were investigated. Ejector lengths of approximately 2.0 standard nozzle diameters and ejector diameters larger than 1.6 standard nozzle diameters provided the greatest additional noise reduction to that obtained with the mixing nozzles alone. The ejector can restore the static thrust loss caused by use of the mixing nozzle or can provide static-thrust augmentation.

The noise reduction obtained from an ejector is a function of the secondary airflow rate and results from the diffusion of the jet to lower velocity. Velocity profiles at the ejector exit are compared with previous results obtained using conical nozzles and with calculated free-jet boundaries resulting from normal spreading at equivalent downstream distances.

Maximum probable noise reductions calculated from weighted local jet velocity and area were not realized probably because the noise generated inside the ejector is appreciable.

INTRODUCTION

Low-flying jet aircraft operating from municipal airports surrounded by residential communities present a formidable noise annoyance problem. In addition to the annoyance factor, however, the fluctuating pressures of the high intensity noise are a source of structural damage to the aircraft. Therefore, from the standpoint of both the annoyance and the

4853

CZ-1

structural damage, reduction of engine noise should be investigated. There are three obvious approaches to the problem:

(1) The takeoff and climb-out pattern of the aircraft can be adjusted to cause the least annoyance (ref. 1). This does not constitute a solution to the problem, but probably will be used to supplement noise reductions achieved by other means.

(2) The engine itself can be made quieter either by engine design changes as suggested in reference 2 for a low-temperature engine or by a change in the engine cycle, such as the bypass engine.

(3) Exhaust-nozzle modifications or other devices that cause less noise to be generated can be added to the engine. This method is applicable to current engines and is the basis for the work reported herein.

Jet engine noise has been shown to be generated by the same processes as the noise from a simple air jet (ref. 3) and arises from the turbulent mixing of the jet with the surrounding atmosphere. The noise generated by this process is a function of the jet velocity to a high power (near eight) and the jet area (ref. 3 and 4). The predominant noise sources may be some distance from the nozzle exit (ref. 5).

Screens placed across the jet near the nozzle exit have yielded large noise reductions (ref. 6). The drag force of the jet on the screen is a large part of the total engine thrust and, therefore, this type of device would not be suitable for flight use. From these tests, however, we may conclude two things: (1) the noise generated inside the engine and immediately downstream (12 in.) is not a large part of the total noise, and (2) spreading the jet and reducing its velocity in a short distance is effective in reducing the noise generated downstream.

Nozzles that have achieved noise suppression with small engine performance penalty, in general, have changed the jet-mixing process by means of multiple or segmented nozzle configurations (refs. 7 to 9). Mixing interference of adjacent jets (ref. 8) and induced airflow between the jets are probably the most important factors affecting noise generation.

The ejector is a device that has shown promise from two important aspects of the noise problem. If the mixing of the induced air of the ejector and the primary jet can be nearly completed within the ejector, the jet issuing from the ejector has higher mass flow, lower temperature, and lower velocity and consequently generates less noise than the primary jet alone. Also, the ejector can be a thrust-augmenting device and can offer at least a partial solution to the thrust losses experienced with other noise-suppression devices.

4853

Previous work on the effect of ejectors on the noise characteristics of an engine with a conical convergent nozzle (ref. 10) showed that the ejector and simple nozzle did not sufficiently alter the mixing process and provided only a 2 decibel noise reduction. However, model tests of combined mixing nozzles and ejectors reported in reference 11 showed that the noise-suppression properties of mixing nozzles could be supplemented by ejectors of moderate length. A combined investigation of the acoustic characteristics and thrust and drag penalties of several full-scale noise-suppressor configurations (ref. 12) included a mixing nozzle with an ejector, which also showed promising results. An extension of this work into the transonic regime is reported in reference 13.

The purpose of the work at the NACA Lewis laboratory reported herein was to study the noise characteristics, the engine performance, and the primary-secondary jet-mixing characteristics of full-scale engines equipped with ejectors and exhaust-mixing nozzles. Two ejector diameters and a range of ejector lengths and ejector to nozzle-spacing distances were investigated. Pressure and temperature surveys at the ejector exit were made and velocity profiles were obtained.

## APPARATUS AND PROCEDURE

### Engines and Test Stands

Two axial-flow turbojet engines with rated sea-level thrusts of approximately 9000 and 5000 pounds were used. The larger engine (9000-lb thrust) is given the designation "engine A" and the smaller engine the designation "engine B" for the data presentation and discussion to follow. Engine A develops its rated thrust at an exhaust-nozzle pressure ratio near 2.3 and at a relatively low exhaust-gas temperature (approximately 900° F). Engine B operates at a lower exhaust-nozzle pressure ratio of 1.7 at rated conditions, but at a higher exhaust-gas temperature (1275° F). As a result, both engines have effective jet velocities of approximately 1750 feet per second at rated thrust.

Engine installations. - Engine A was mounted in an outdoor thrust stand as shown in figure 1. The centerline of the engine was 8 feet above ground level. A large bellmouth inlet section was used to provide undistorted airflow at the compressor inlet, and a large screen at the bellmouth entry prevented ingestion of foreign material. An acoustic panel of perforated metal and glass fiber material backed with cement board was placed in front of the engine to reduce compressor noise annoyance in nearby buildings.

Engine B was one that had been installed previously in the thrust stand for the acoustic study reported in reference 8 and, therefore, the acoustic and performance characteristics were well established. For this

investigation, however, the engine was installed in an airframe shown in figure 2 and was operated using the existing fuel, lubrication, and control systems.

Engine instrumentation. - Thrust measurements for both engines were made by means of temperature-compensated strain-gage tension links. For the engine A installation, the thrust link was a part of the thrust stand. For engine B the link was located in the restraining cable shown in figure 2.

Airflow measurement instrumentation (static-pressure rakes and wall taps) was installed in the cylindrical section of the bellmouth inlet on engine A. Fuel flow to the thrust stand was measured by a turbine-type flowmeter. No airflow or fuel-flow instrumentation was provided for engine B in the airframe. However, since engine airflow is a function of engine speed and is essentially independent of the exhaust section, the airflow was calculated for the standard conical nozzle and the resulting calibration curve was used for the other nozzle configurations.

Engine speed and exhaust-gas temperature and pressure were measured for both engines.

Engine operation. - The engines were operated over a range of power settings from approximately 50 to 100 percent of rated thrust. Engine performance data (thrust, speed, etc.) were obtained at up to five engine power conditions. Performance parameters were obtained and comparisons between the various configurations and the standard conical convergent nozzles were made for each engine.

#### Exhaust Nozzles and Ejectors

Exhaust nozzles designed to promote mixing and hasten diffusion of the jet, both when used alone and in conjunction with ejectors, were made for each engine. The mixing nozzles had slightly greater exhaust areas than the conical convergent standard nozzle for each engine and included provision for the addition of area trim to match the operating characteristics of the respective standard nozzles. Nozzle and ejector dimensions are given in table I.

Lobe nozzles. - A 12-lobe nozzle, shown in figure 3(a) and previously used in a thrust, drag, and acoustic characteristics investigation (ref. 12) was installed on engine A. The nozzle with an ejector is shown in the photograph and sketches in figure 3(b).

An 8-lobe nozzle with an ejector (fig. 3(c)) was used with engine B. The over-all diameters of the 8- and 12-lobe nozzles were nearly equal, but the exhaust-gas passage was almost 20 percent less for the 8-lobe nozzle because of the engine size relation.

Centerbody nozzle with radial airjets. - A nozzle designed to spread the jet by means of radial airjets issuing from a centerbody is shown in figure 4, and was used with engine A. This configuration has a conical convergent nozzle with a protruding centerbody. The centerbody is a plenum chamber connected by four supply lines to the high-pressure compressor bleed ports of the engine. Two centerbody tip sections were used, each having eight convergent-divergent nozzles with exit diameters of 1.0 inch. The nozzles were designed to bleed 5 percent of the engine airflow with a bleed-jet Mach number of 2.0. In one centerbody tip, the nozzles discharged perpendicular to the jet (normal to the cylindrical section of the centerbody) at the plane of the exhaust-nozzle exit. In the other centerbody tip, the nozzles were positioned further downstream on the centerbody so that the nozzles (normal to a curved section of the centerbody) were canted back approximately  $15^\circ$  from a perpendicular position to the engine exhaust jet.

Ejectors. - Two ejectors with telescopic cylindrical sections and flared inlets were used in the investigation. The configurations used together with the range of each variable studied are shown in table I. Dimensions are given in terms of standard-circular-nozzle diameters for each engine.

To determine the extent of the mixing of the primary jet and secondary airflow through the ejector, surveys of the pressure and temperature distributions at the ejector exits were made using thermocouple and total-pressure rakes as shown in figure 3(c). The rakes were installed radially inward from the exit rim of the ejector. The rakes were located directly downstream of both the lobes and valleys of the lobe-type nozzles (figs. 3(b) and (c)).

#### Acoustic Measurements

The acoustic terms and symbols used herein are defined in the appendix. Sound-level measurements were made with a commercial sound-level meter and a condenser microphone. Frequency distributions were measured using an automatic audio frequency analyzer and recorder also equipped with a condenser microphone. The analyzer was mounted in an acoustically insulated truck and direct field records were taken. Both instruments were calibrated before each test using a small loudspeaker-type calibrator and transistor oscillator.

Acoustic measurements for both engines were made in  $15^\circ$  increments at a radial distance of 200 feet. The sound field for engine A is shown in figure 5. Measurement stations were located over a  $225^\circ$  sector and extended from  $90^\circ$  from the jet axis on one side to  $135^\circ$  from the jet axis on the other side of the engine. No measurements were made in the quadrant in which the control building was located, nor forward of the engine

in the predominantly compressor-noise region, which was shielded by the acoustic panels. The sound field for engine B was similar except that measurements were made on one side of the engine only over the region from  $15^{\circ}$  to  $135^{\circ}$  from the jet axis.

The sound fields were free from large reflecting surfaces other than the ground (turf and concrete) and the nearest large building was located approximately 500 feet in front of the engines.

Sound pressure level measurements were made at each measurement station for several power conditions for each configuration. Spectrum levels were obtained at all the measuring stations on one side of the engine only.

## RESULTS

The results obtained for the various noise-suppressor configurations are presented in the following order: (1) acoustic, (2) jet mixing, and (3) engine performance. The effectiveness of the various mixing nozzle-ejector combinations in satisfying the design objectives are determined in comparison with the results obtained for a standard conical convergent nozzle and for the noise suppressor without an ejector. Some of the effects of variables such as engine thrust, ejector length, and spacing distance are also shown.

### Acoustic

The acoustic results obtained are presented in the form of (1) polar plots showing the directional distribution of the sound pressure about the engine, (2) spectrum level distribution at three azimuths,  $30^{\circ}$ ,  $90^{\circ}$ , and  $135^{\circ}$  from the jet axis, and (3) power spectrum level distribution.

The use of the engine parameters, thrust, engine speed, or pressure ratio, as a basis for the acoustic comparisons is made undesirable by variable engine and ambient conditions over the period of the investigation. Engine deterioration, suppressor nozzle discharge coefficient, nozzle area changes, differences among individual engines, and seasonal changes can become large factors in the tabulation of acoustic results. The primary variable in jet-noise generation is jet velocity and, therefore, all of the acoustic results presented have been corrected to a jet velocity of 1700 feet per second. Corrections were made based on the relation of sound power level to jet velocity for each configuration and in most cases involved interpolation rather than extrapolation of the data. Corrections to spectra and polar plots assumed equal level shifts at all frequencies and azimuths. The amount of the correction was in no case



more than 3 decibels and was generally less than 2 decibels. Values obtained from the measurements on each side of the engine have been averaged to compensate for wind effects.

12-Lobe nozzle and ejector. - Figure 6 shows the results obtained for the standard engine A configuration, the 12-lobe nozzle, and the 12-lobe nozzle with one of the ejector configurations that gave the greatest noise reduction.

Figure 6(a) presents the directional distribution of the sound pressure level and shows a reduction at the maximum points ( $30^\circ$ ) of 3 decibels for the suppressor nozzle alone and 9 decibels for the nozzle-ejector combination. The occurrence of the maximum reduction in sound pressure level at approximately a  $45^\circ$  position is characteristic of much of the data obtained with ejectors. Sound power level reductions of 3 decibels for the 12-lobe nozzle and an additional reduction of nearly 5 decibels for the 12-lobe nozzle-ejector combination were obtained for a total of approximately 8 decibels.

Spectrum levels for the 12-lobe nozzle and 12-lobe nozzle with ejector are shown in figures 6(b), (c), and (d). At the  $30^\circ$  azimuth (fig. 6(b)), the lobed nozzle yielded reductions of 5 to 13 decibels over the frequency range of from 160 to 1000 cycles per second. When combined with an ejector, sound power level reductions of 13 to 23 decibels were obtained in the frequency range from 200 to 5000 cycles per second. The spectra at azimuths of  $90^\circ$  and  $135^\circ$  to the jet (figs. 6(c) and (d)) show small reductions throughout the middle range of frequency with some increase at the higher frequencies for the noise-suppressor configurations.

Power spectrum level distribution is shown on figure 6(e). The mixing nozzle alone caused reductions at all frequencies below 1200 cycles per second and slight increases at the higher frequencies. The addition of the ejector resulted in reduced power spectrum levels at all frequencies. The maximum reduction was 10.5 decibels at 200 cycles per second.

The effects of three ejector parameters (diameter, length, and spacing distance) on noise generation are shown in figure 7. In each case, one parameter is varied and two others are held constant. All the parameters are presented in terms of standard nozzle diameters. The effect of ejector diameter (fig. 7(a)) is of considerable interest. The smaller diameter ejector ( $D_2/D_1 = 1.4$ ) gave a reduction in sound power level of nearly 6 decibels and the larger diameter ejector ( $D_2/D_1 = 1.7$ ) shows nearly an 8-decibel reduction. The difference is a result of reductions almost entirely in the direction of maximum sound pressure level. The maximum reduction (11 db) in sound pressure level occurred at the  $45^\circ$  azimuth.

Directional distribution of sound pressure as a function of ejector length is shown in figure 7(b). These data indicate that an ejector

length of at least 2 nozzle diameters is necessary to obtain significant noise reduction.

Spacing distance (nozzle exit to ejector inlet) is seen in figure 7(c) to have only a slight effect on noise generation. Total variation over the range of  $S/D_1$  investigated was slightly over 1 decibel in sound power level.

The variation in noise generation as a function of engine thrust is shown in figure 8 for a 12-lobe nozzle and ejector configuration. Some ejector configurations (ref. 8) have shown resonant characteristics at certain operating conditions that resulted in noise level increases. None of the ejector configurations used with the lobed nozzles showed any such characteristics at any engine speed.

8-Lobe nozzle. - Noise suppression characteristics of the 8-lobe nozzle and the nozzle-ejector combination on engine B are compared with the standard configuration in figure 9. The reduction in maximum sound pressure levels obtained from the use of the 8-lobe nozzle alone was 7 decibels (fig. 9(a)). An additional reduction in the maximum point ( $45^\circ$  to  $60^\circ$ ) of 4.5 decibels was obtained from the ejector for a total of almost 12 decibels. Reductions in sound power level of 4 decibels for the 8-lobe nozzle and 8 decibels for the nozzle-ejector combination were obtained. The use of the ejector with this nozzle results in decreased sound power levels at the sides and forward of the engine averaging over 3 decibels. The spectrum level distribution (fig. 9(b)) shows reductions at the  $30^\circ$  azimuth for the entire frequency range (over 19 db at 1000 cps). At the side and forward azimuths the reductions were less in the mid-frequencies and increases occurred at frequencies over 3000 cycles per second. The frequency distribution of sound power level (fig. 9(e)) shows reductions at all frequencies. Reductions of 5 to 11 decibels occurred for all frequencies between 80 and 2500 cycles per second.

Directional distribution of sound pressure level for three ejector lengths is shown in figure 10(a). Increasing the ejector length from 1.64 to 2.13 diameters results in sound pressure level reductions of 2 to 3 decibels at all azimuths. Further increase in length to 2.44 diameters did not appreciably affect the results. Frequency distributions of sound power (fig. 10(b)) for ejector lengths of 1.64 and 2.44 diameters show similar characteristics with the greater ejector length (2.44 diameters) yielding additional reductions of 2 to 6 decibels over a range of frequencies from 80 to 2500 cycles per second.

Centerbody bleed nozzle. - The acoustic characteristics of the centerbody bleed nozzle were not good, and after determining that the over-all performance was not satisfactory the tests were discontinued. The results obtained showed only a slight rearward noise reduction from that of the standard configuration and also showed slightly increased

sound levels forward. The configuration with the canted nozzles and ejector gave the best results and it was less than 1.0 decibel lower in over-all sound power level than the standard nozzle at the same thrust.

### Jet Mixing

Previous work (ref. 10) had shown that for conical nozzles and ejectors with diameter ratios of 1.2 and 1.4, the noise generation was a function of the primary jet velocity. This was true because the primary jet was essentially unaltered. Normal spreading of the jet would have produced very nearly the same velocity profiles at an equivalent distance downstream of the nozzle exit. Measured jet velocity boundaries (ref. 5) for a turbojet engine similar to engine A yielded a normal jet-spreading angle of slightly less than  $7^\circ$  from the jet axis.

12-Lobe nozzle. - Velocity profiles for the 12-lobe nozzle and ejector are compared with those of reference 10 in figure 11. The velocity profiles are presented in terms of the ratio of the local velocity at the ejector exit to the effective jet velocity. The effective jet velocity is the engine thrust divided by the mass-flow rate through the engine and provides a bulk velocity term that is applicable for both subsonic and supersonic jets. Included in figure 11 are the calculated boundaries of jets at equivalent distances downstream for a jet-spreading angle of  $7^\circ$ . Profiles for both the region axially downstream of a nozzle lobe and downstream of a space between lobes are shown.

The abscissa used for figure 11 is  $(d_2/D_1)^2$  which is equivalent to the ratio of the areas of concentric circles through the point of measurement to the area of the standard nozzle. The zero velocity intercept for each curve represents the physical boundary of the ejector. Of significance in figure 11 is the fact that the data for the 12-lobe mixing nozzle and ejector show that the jet filled the ejector and therefore covered an area 25 percent greater than would result from normal spreading. The maximum jet velocity was reduced to 1150 feet per second as compared with an effective jet velocity at the nozzle of almost 1600 feet per second ( $v_2/V_{eff} = 0.72$ ). In addition, the smaller ejector of reference 10 ( $D_2/D_1 = 1.2$ ) is shown in figure 11 to actually restrict the normal spreading of the jet ( $(d_2/D_1)^2 = 1.44$  at ejector shell, whereas for normal spreading  $(d_2/D_1)^2 = 1.88$  for  $L/D_1 = 1.5$ ). The larger ejector of reference 10 showed almost no effect on jet spreading.

The ejector was not rigidly supported and flexing of the supports was possible and did occur. Under some conditions, changes in jet attachment caused movement of the ejector. Therefore, successive tests did not always give repetitive velocity profiles. In addition, rotational shifts of the profiles for the lobes and the spaces between the lobes

occurred. However, mixing was well advanced as evidenced by the fact that the differences between the two profiles were small. Calculations of the secondary airflow based on integrated velocity profiles showed the secondary- to primary-weight-flow ratios to be nearly 0.9 at high engine power.

8-Lobe nozzle. - Ejector exit velocity distribution profiles obtained for the 8-lobe nozzle are shown in figure 12 in the same dimensionless form used for the 12-lobe nozzle. The velocity distribution was measured at four engine thrust conditions, but the variation with thrust was negligible and only one set of data is presented. The jet boundary for a circular jet spreading  $7^\circ$  from the jet axis for a distance equal to the ejector length is shown in figure 12. The profiles (fig. 12) show that diffusion of the jet to approximately 9 percent greater than normal area was obtained. The sharp peaks near the ejector shell result from the divergence angle of the lobes and indicate that the ejector diameter might be increased for further diffusion. The ejector was rigidly mounted to the nozzle and the profiles for successive tests were similar.

#### Engine Performance

A noise suppressor, which functions by providing increased mixing of the jet and surrounding air, suggests penalties in the form of thrust losses and drag increases. The use of an ejector as a part of a suppressor has demonstrated two features: (a) statically and at low forward speeds, the forward-facing surfaces of an ejector are subjected to pressure forces in the thrust direction and (b) the pressure forces reverse with increasing forward speed until at cruise flight speeds the force in the drag direction may be an appreciable part of the propulsive thrust (refs. 12 and 13). Both the characteristics, thrust augmentation and drag, depend upon the area of and the pressure distribution on the forward-facing surfaces of the ejectors.

Engine A; 12-lobe nozzle and ejector. - The effect of the noise-suppressor configurations on engine performance is shown in figure 13 in the form of a thrust coefficient ratio

$$\frac{\text{Suppressor nozzle thrust coefficient}}{\text{Standard nozzle thrust coefficient}}$$

as a function of the nozzle pressure ratio. This method essentially evaluates the nozzle independently of the engine and ambient conditions. Figure 13(a) shows the results obtained for the 12-lobe nozzle-ejector configuration for two ejector diameter ratios. The thrust coefficient difference shown in figure 13 is probably due more to the difference in the areas of the forward-facing surfaces at the ejector inlet than to the difference in exit diameters. The thrust augmentation of the larger

ejector is as much as 4 percent based on the suppressor nozzle and results in a thrust increase of 2 percent above that of the standard nozzle.

Ejector length is an important parameter in determining the secondary airflow rate and acoustic characteristics of an ejector and, as shown in figure 13(b), the ejector length also has considerable effect on the static thrust coefficient. The short ejector is seen to be ineffective at low-jet-pressure ratios.

A consistent and significant increase in thrust coefficient ratio with the spacing distance is shown in figure 13(c). Thrust coefficient ratio increases (based on the mixing nozzle) on the order of 2 to 4 percent occurred over the range of spacing distances and pressure ratios investigated.

Engine B; 8-lobe nozzle and ejector. - Thrust coefficient ratios ( $C_F/C_{F_{std}}$ ) corrected for mass flow and jet velocity were calculated for the 8-lobe nozzle configurations (fig. 14) for two values of nozzle pressure ratio. At the higher pressure ratio (1.6) the thrust augmentation is approximately 5 percent based on the standard nozzle configuration and approximately 8 percent based on the suppressor nozzle. No significant trend of thrust augmentation with ejector length was evidenced.

## DISCUSSION

### Jet Mixing and Noise Reduction

A method for determining what is probably the maximum possible noise reduction for mixing nozzles is presented in reference 14. The method assumes complete mixing of the jet and a secondary mass flow of air, which depends upon the geometry of the noise suppressor. At some distance downstream, the mixed jet and air are assumed to have the characteristics of a larger jet at a lower and uniform velocity. For an ejector configuration, the mixed jet area would be the ejector exit area. A noise reduction near 20 decibels is predicted for an ejector of the size reported herein. This predicted 20-decibel noise reduction assumes a uniform velocity profile.

With a nonuniform velocity profile at the ejector exit such as shown in figure 11 for the experiments reported herein (maximum jet velocity, 1150 ft/sec; mean jet velocity, 866 ft/sec for the 86 percent rated thrust condition), the measured noise reduction would be expected to be less than the maximum reduction predicted from reference 14.

If we can consider the noise generation of each part of the jet to be a function of the eighth power of the local jet velocity, then by integration (over the exit area) of the velocity profile raised to the eighth power we can determine a weighted area and velocity term. A value of the noise reduction can be determined from the ratio of  $AV^8$  for the ejector configuration and the standard nozzle. Using the relation  $PWL = 10 \log_{10} A_{std} (V_{std})^8 / AV^8$ , a value of 12.5 decibels is obtained for the expected noise reduction. The configuration for which the velocity-profile data were presented had a total sound power reduction of approximately 7 decibels. The difference probably is due to the following reasons: (1) the noise generated by the mixing inside the ejector is not negligible and (2) while airjets and engines in general follow the eighth power variation, specific engines may have a somewhat lower exponent for their jet velocity-noise relation.

The lobe nozzle and ejector combination has been shown (fig. 11) to result in increased jet mixing and reduced maximum velocity. The decrease in maximum jet velocity is probably the primary reason for the noise reduction. This is in agreement with the results reported in references 10 and 15, which indicated that maximum jet velocity is the predominant factor in noise generation and that reduction in viscous shear by reduced velocity gradient produced only a moderate effect on noise generation.

Approximately equivalent noise reduction characteristics were obtained with the 8- and 12-lobe nozzle and ejector combinations. The increased initial jet spreading of the 8-lobe nozzle (by virtue of the large envelope diameter in proportion to the exhaust-gas flow rate) resulted in effective noise suppression at somewhat lower values of  $L/D_1$  and  $D_2/D_1$  for this nozzle.

#### Noise Suppression and Engine Performance

An examination of figures 7, 10, 13, and 14 shows that maximum noise reduction and maximum thrust ratio are obtained from the configurations with the longer ejectors. Both the noise reduction and the thrust augmentation are functions of the secondary mass flow through the ejector, and the mass-flow ratio is a function of ejector length. The optimum length is determined by frictional forces, which limit the mass-flow ratio. The acoustic and thrust characteristics indicate that the optimum ejector length probably is near the maximum length tested for both engines. The effect of increased mass flow is to increase the ejector inlet velocity, which results in reduced pressure on the forward-facing surfaces of the ejector creating the thrust force. Improved mixing and reduced maximum jet velocity result in greater noise reduction.

Increase in the ejector spacing distance (ejector moved aft) improved the thrust ratio but did not show any significant change in the acoustic characteristics. With the ejector near the nozzle, a drag force is generated on the rearward-facing surfaces of the nozzle by the same mechanism that results in a thrust-augmentation force on the forward-facing surfaces of the ejector. As the ejector was moved aft, the velocity of the secondary air over the rearward-facing nozzle surfaces (spaces between lobes) was diminished, the static pressure was increased, and the drag force was reduced.

#### CONCLUDING REMARKS

An ejector combined with a lobe nozzle diffuses the jet exhaust to a lower velocity and results in reduced noise levels. Sound pressure level reductions of 12 decibels and sound power level reductions of 8 decibels were obtained. The ejector provides approximately 3 to 5 decibels of the sound power reduction.

Ejector lengths of approximately 2.0 standard nozzle diameters and ejector diameters over 1.6 standard nozzle diameters provided significant additional noise reduction to that obtained with the lobe nozzle alone.

Maximum velocity at the ejector exit is the most important parameter in the noise generation. Calculations of the theoretical noise reduction based on local flow conditions at the ejector exit yielded noise reduction values considerably greater than were measured experimentally. Noise generated inside the ejector by the mixing of the jet and secondary air probably accounts for most of the noise reduction differences.

Static-thrust augmentation and noise reduction were both functions of secondary mass-flow rates as evidenced by their dependence upon ejector length.

Factors that result in static-thrust augmentation can become sources of cruise flight drag increase. Therefore, retraction of the entire ejector or of the static thrust augmenting surfaces may be necessary.

Lewis Flight Propulsion Laboratory  
National Advisory Committee for Aeronautics  
Cleveland, Ohio, May 27, 1958

## APPENDIX - NOMENCLATURE

## Acoustic Terms

The decibel is a dimensionless unit for expressing the ratio of two powers. Ratios of other quantities (such as pressure, voltage, etc.) that are square roots of corresponding power ratios may also be expressed in decibels. Sound pressure level, spectrum level, power level, and power spectrum level are presented in decibel units.

Sound pressure level. - Sound pressure level (SPL) is 20 times the  $\log_{10}$  of the ratio of the root mean square sound pressure at a point to a reference pressure of  $2 \times 10^{-4}$  dynes per square centimeter.

Over-all sound pressure level. - The over-all sound pressure level (all frequencies simultaneously) is obtained directly from the sound level meter using the flat frequency response setting.

Spectrum level. - The spectrum level is the sound pressure level within a specified frequency band of 1 cycle per second width.

Sound power level. - Sound power level (PWL) is 10 times the  $\log_{10}$  of the ratio of the total acoustic power radiated from a source to a reference power of  $10^{-13}$  watts. The acoustic power is obtained from an integration process (refs. 16 and 17) of the sound pressure levels over a hemispherical region surrounding the noise source.

Power spectrum level. - The power spectrum level is the power level at a specified frequency band of one cycle per second width.

## Symbols

A	area
$C_F$	thrust coefficient
D	diameter
$D_1$	diameter of exit of standard nozzle or conical convergent nozzle of area equivalent to mixing nozzle. Engine A, $D_1 = 21.7$ in.; Engine B, $D_1 = 19.5$ in.
$D_2$	diameter of ejector
d	diametric distance (origin on the jet axis)
F	net thrust



L distance from nozzle exit to ejector exit  
m mass-flow rate through engine  
r radius, in.  
S spacing distance, nozzle exit to ejector inlet  
V velocity  
 $V_{\text{eff}}$  effective velocity, F/m  
 $v_2$  local velocity at ejector exit

## Subscripts:

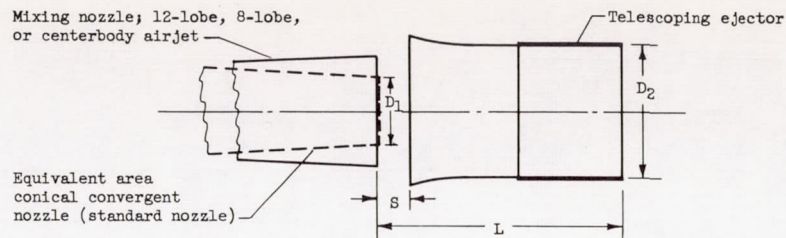
corr corrected  
max maximum  
std standard  
1 nozzle exit  
2 ejector exit

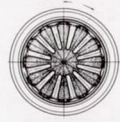
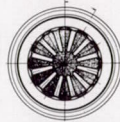
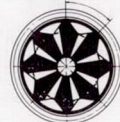
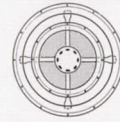
## REFERENCES

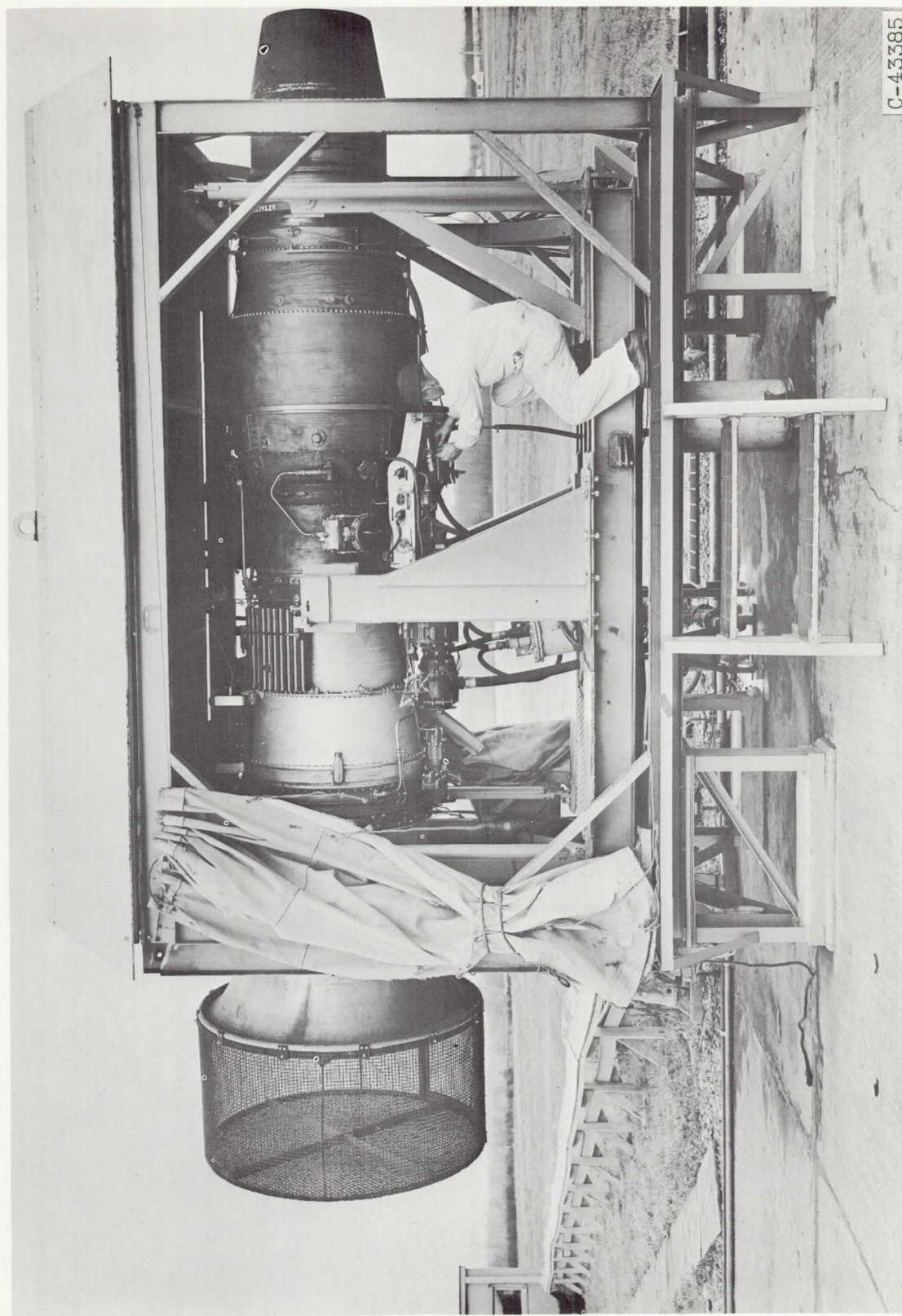
1. North, Warren J.: Effect of Climb Technique on Jet-Transport Noise. NACA TN 3582, 1956.
2. Silverstein, Abe, and Sanders, Newell D.: Concepts on Turbojet Engines for Transport Application. Preprint No. 727, SAE, 1956.
3. Coles, Willard D., and Callaghan, Edmund E.: Investigation of Far Noise Field of Jets. II - Comparison of Air Jets and Jet Engines. NACA TN 3591, 1956.
4. Lighthill, M. J.: On Sound Generated Aerodynamically. I - General Theory. Proc. Roy. Soc. (London), ser. A., vol. 211, no. 1107, Mar. 20, 1952, pp. 564-587.
5. Howes, Walton L., and Mull, Harold R.: Near Noise Field of a Jet-Engine Exhaust. I - Sound Pressures. NACA TN 3763, 1956.
6. Coles, Willard D., and North, Warren J.: Screen-Type Noise Reduction Devices for Ground Running of Turbojet Engines. NACA TN 4033, 1957.

7. Greatrex, F. B.: Jet Noise. Preprint No. 559, Inst. Aero. Sci., 1955.
8. Coles, Willard D., and Callaghan, Edmund E.: Full-Scale Investigation of Several Jet-Engine Noise-Reduction Nozzles. NACA TN 3974, 1957.
9. Withington, Holden W.: Silencing the Jet Aircraft. Aero. Eng. Rev., vol. 15, no. 4, Apr. 1956, pp. 56-63; 84.
10. North, Warren J., and Coles, Willard D.: Effect of Exhaust-Nozzle Ejectors on Turbojet Noise Generation. NACA TN 3573, Oct. 1955.
11. Miller, M. M.: Sound and Furor - The Jet Noise Suppression Age. Preprint 818, SAE, 1956.
12. Ciepluch, Carl C., North, Warren J., Coles, Willard D., and Antl, Robert J.: Acoustic, Thrust, and Drag Characteristics of Several Full-Scale Noise Suppressors for Turbojet Engines. NACA TN 4261, 1958.
13. North, Warren J.: Transonic Drag of Several Jet-Noise Suppressors. NACA TN 4269, 1958.
14. Dyer, Ira, and Franken, Peter A.: Noise Reduction of a Jet with Mixing. Appendix 1 of Aerodynamic Noise; Its Generation and Suppression by Peter J. Westervelt. Rep. 57GL222, Gen. Eng. Lab., GE, July 1957.
15. Powell, A.: The Influence of the Exit Velocity Profile on the Noise of a Jet. The Aero. Quarterly, vol. IV, pt. 4, Feb. 1954, pp. 431-360.
16. Bolt, R. H., Lukasik, S. J., Nolle, A. W., and Frost, A. D., eds.: Handbook of Acoustic Noise Control. Vol. I. Physical Acoustics. Tech. Rep. 52-204, Aero. Medical Lab., WADC, Dec. 1952. (Contract AF 33(038)-20572.)
17. Callaghan, Edmund E., and Coles, Willard D.: Investigation of Jet-Engine Noise Reduction by Screens Located Transversely Across the Jet. NACA TN 3452, 1955.

TABLE I. - NOZZLE AND EJECTOR DIMENSIONS



Con-figuration	Engine	$D_1$ , in.	$D_2/D_1$	$S/D_1$	$L/D_1$	Design details on figure-	Acoustic data on figure-	Velocity profiles on figure-	$\Delta SPL_{\max} = (SPL_{\text{std}})_{\max} - SPL_{\max}$ , db	$\Delta SPL$ at $30^\circ$ azimuth, db	$\Delta FWL$ , db	Maximum thrust coefficient ratio, $(CF/CF_{\text{std}})_{\max}$	Exit sketch
12-Lobe nozzle	A	21.7				3(a)	6		3.0	3.0	3.0	0.98	
12-Lobe nozzle plus ejector	A	21.7	1.42	0.07 to 0.30	2.59 to 2.91	3(b)	7		5.5	5.5	5.5	1.015	
			1.70	-0.28 to 0.23	1.38 to 2.89	3(b)	6,7,8	11	9.0	9.0	8.0	1.035	
8-Lobe nozzle	B	19.5				3(c)	9		7.0	9.0	4.0	0.97	
8-Lobe nozzle plus ejector	B	19.5	1.60	0.10	1.64 to 2.44	3(c)	9,10	12	12.0	12.0	8.0	1.09	
Center-body airjet plus ejector	A	21.7	1.70	0	2.3	4							



C-43385

Figure 1. - Engine A in thrust stand.

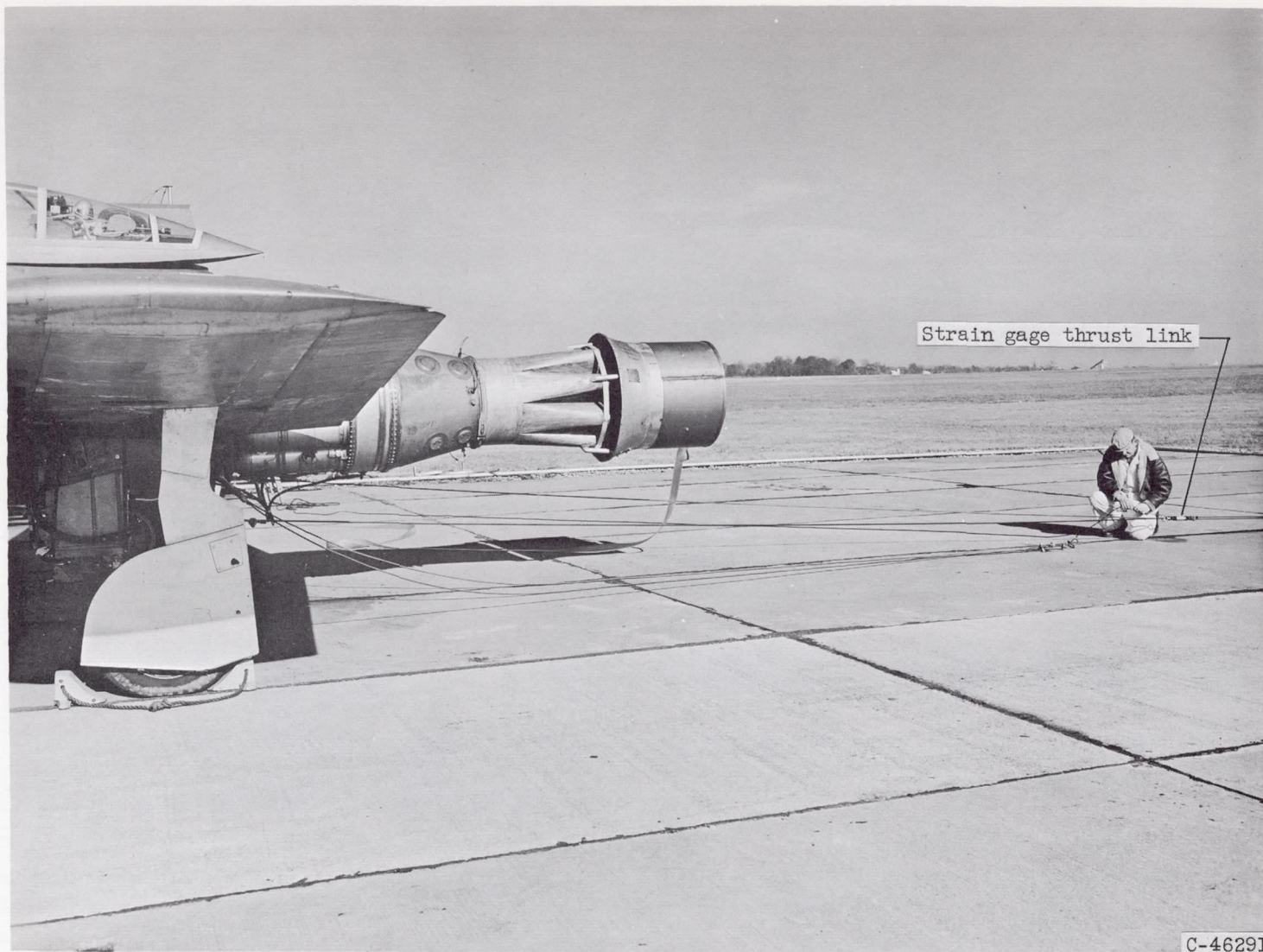
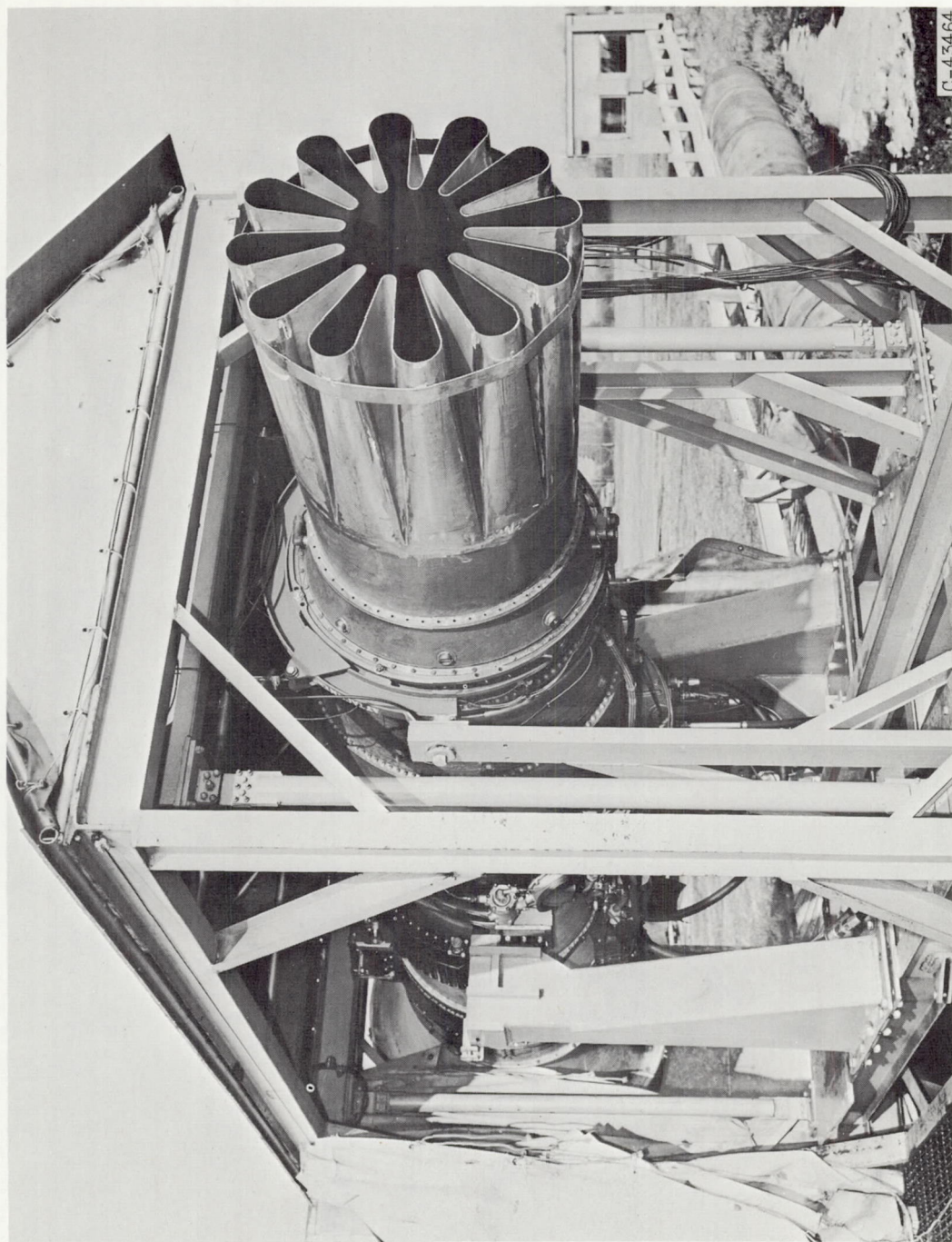


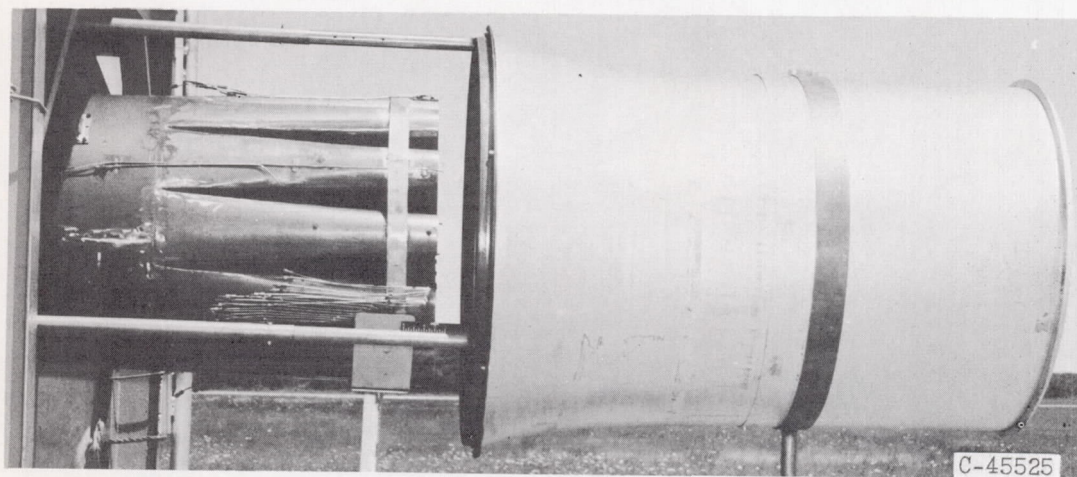
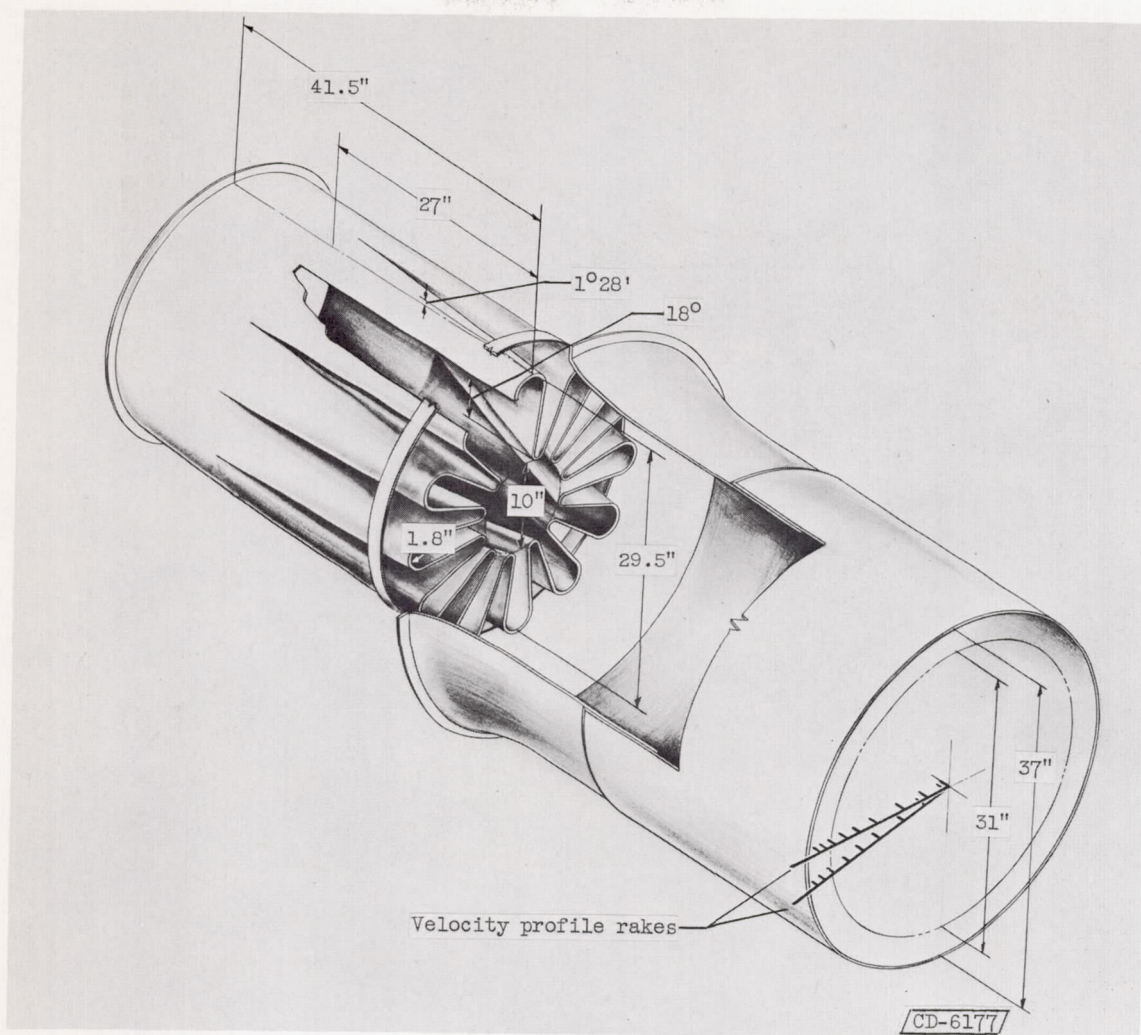
Figure 2. - Engine B in airframe test bed.



(a) 12-Lobe nozzle installed on engine A.

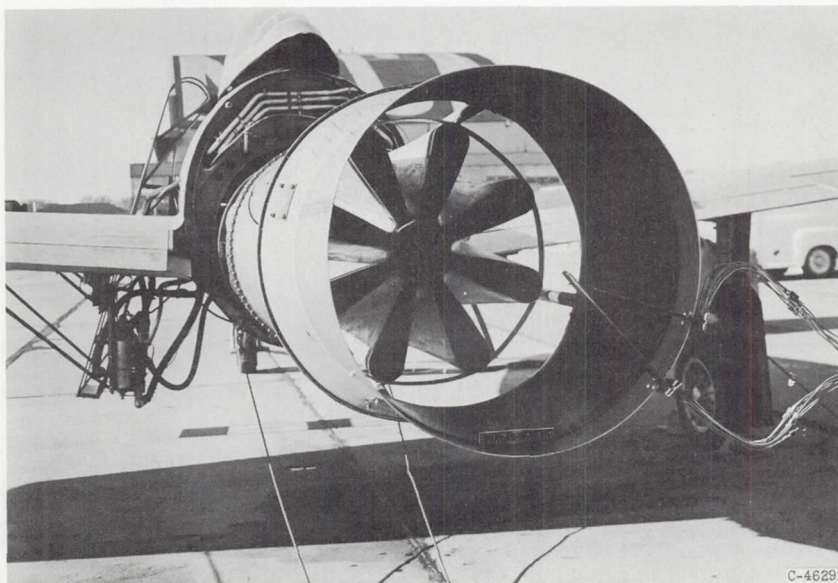
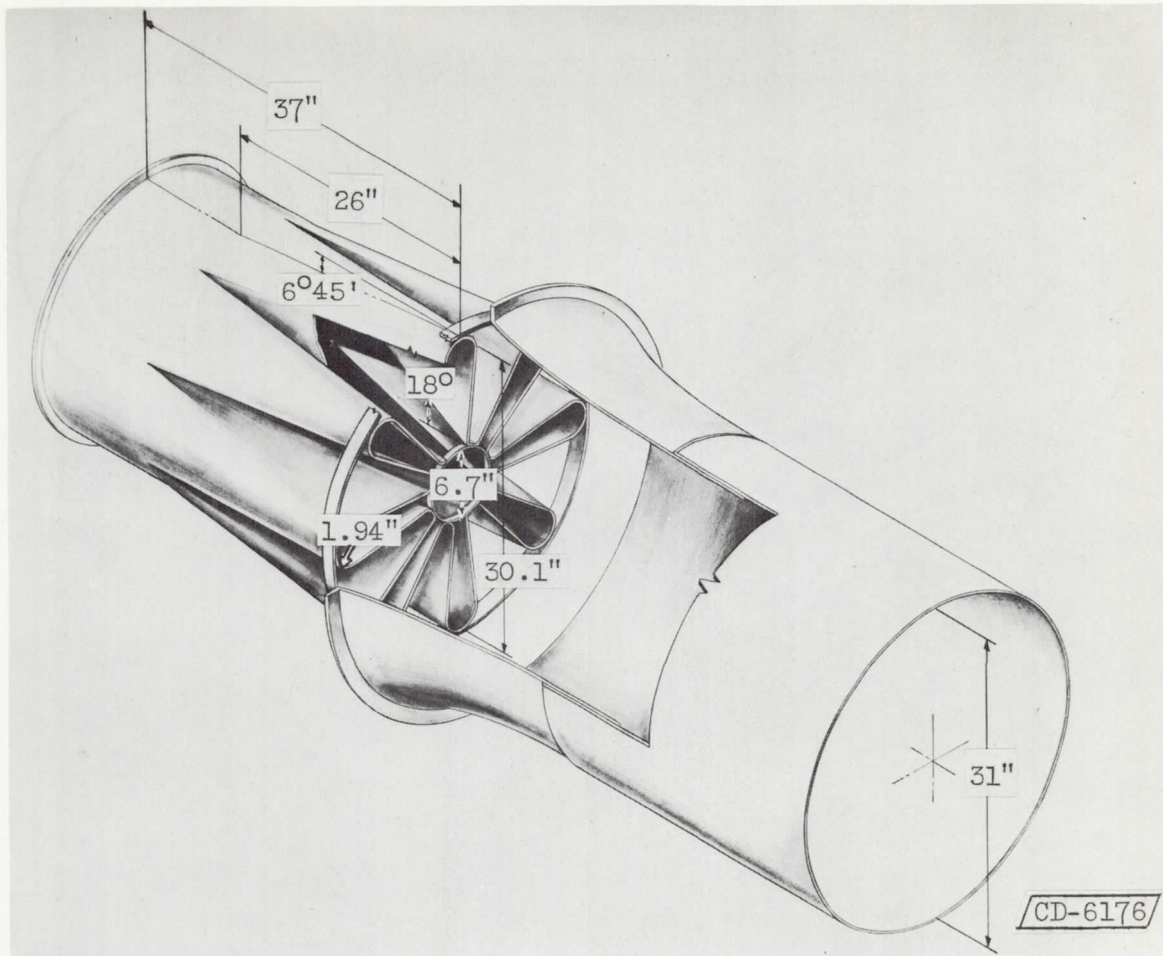
Figure 3. - Lobe-nozzle configurations.

4853



(b) 12-Lobe nozzle and ejectors installed on engine A.

Figure 3. - Continued. Lobe-nozzle configurations.



(c) 8-lobe nozzle with ejector installed on engine B.

Figure 3. - Concluded. Lobe-nozzle configurations.



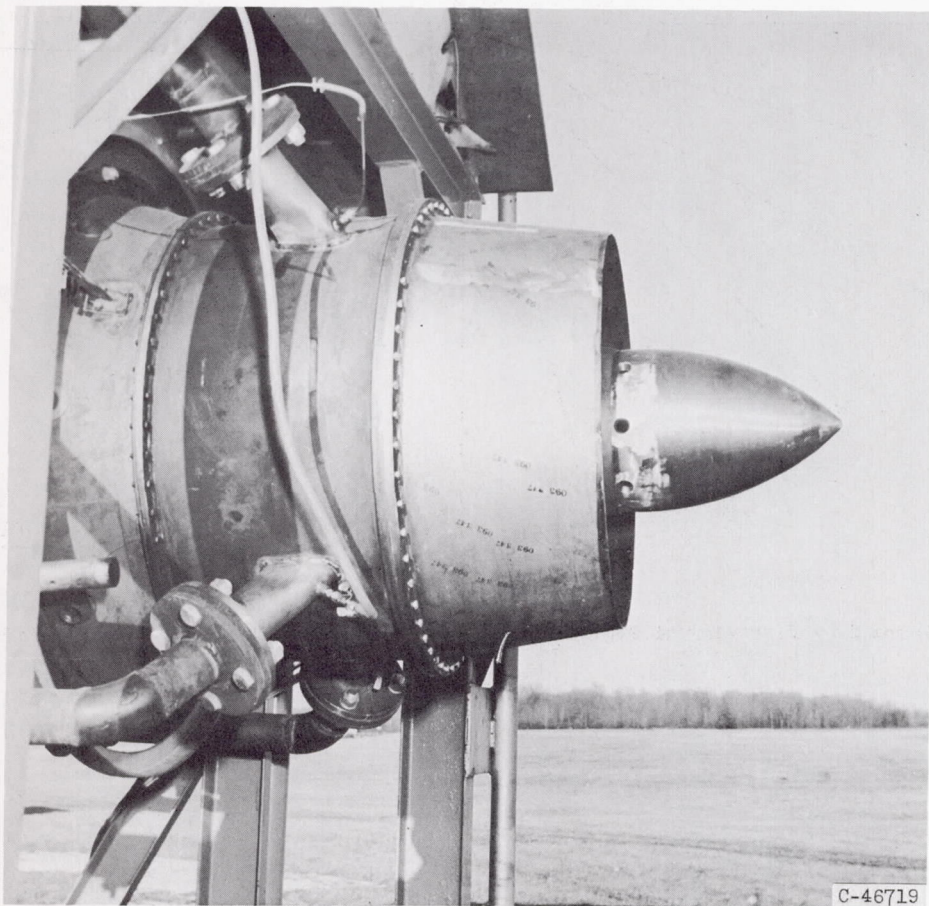
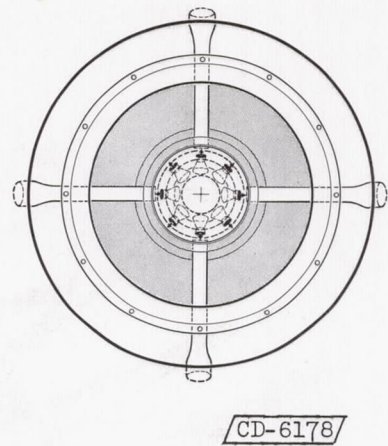
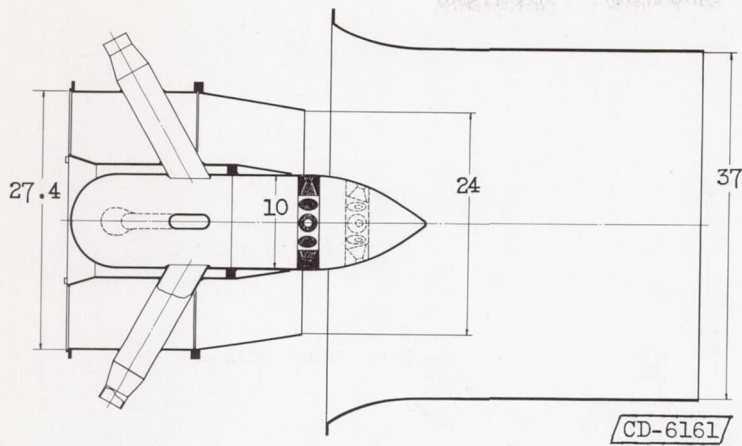


Figure 4. - Centerbody nozzle with radial airjets installed on engine A.  
 (All dimensions in inches.)

4853

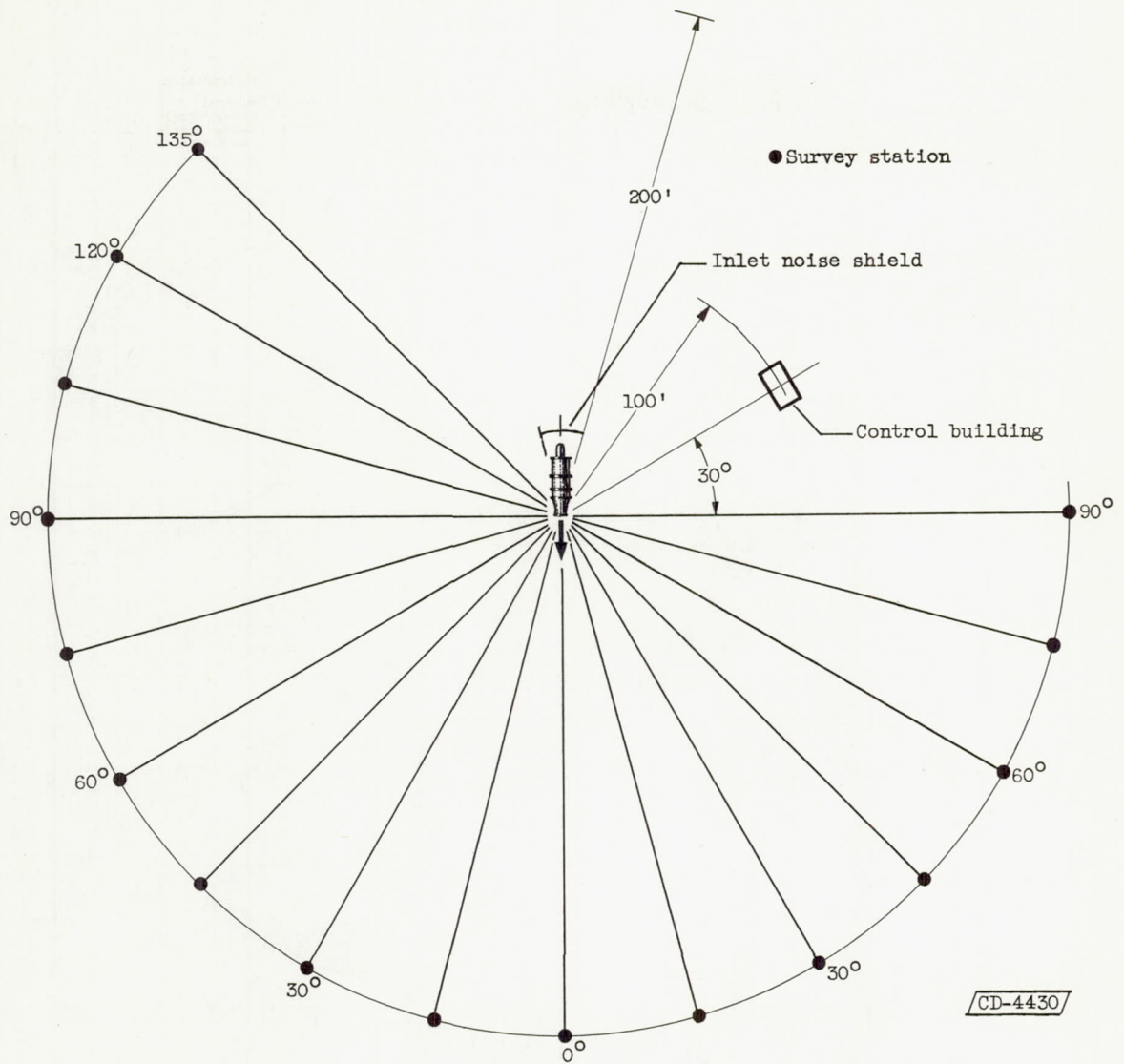


Figure 5. - Plan view of engine A sound survey stations and control buildings.

4853

CZ-4

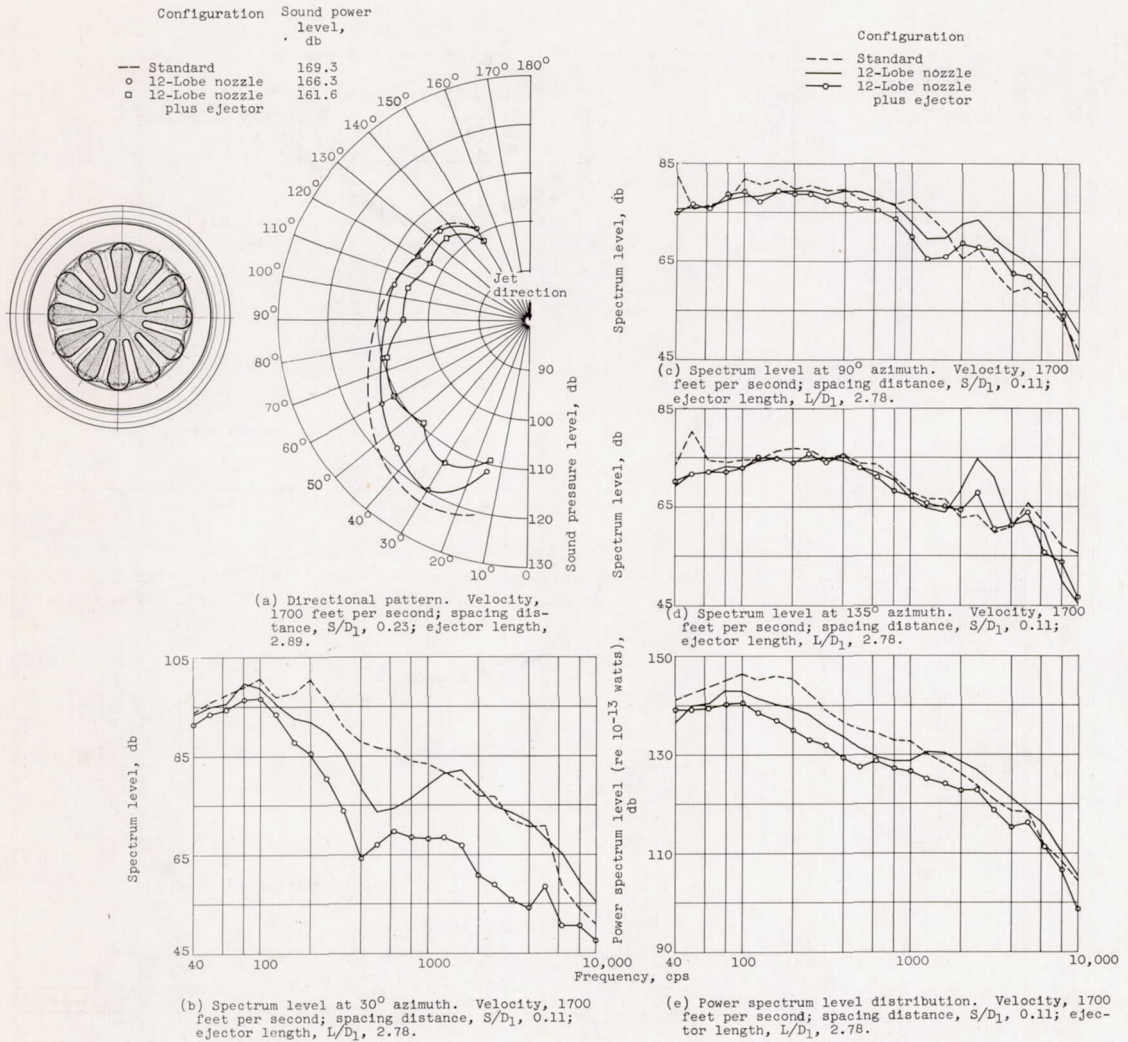


Figure 6. - Acoustic characteristics of 12-lobe nozzle and ejector on engine A. Ejector diameter ratio,  $D_2/D_1$ , 1.7.

Ejector diameter ratio, $D_2/D_1$	Sound power level, db	Ejector length, $L/D_1$	Sound power level, db	Spacing distance, $S/D_1$	Sound power level, db
○ 1.4	163.6	○ 1.38	166.25	○ -0.28	162.2
□ 1.7	161.6	□ 2.25	164.05	□ -.18	162.5
		◇ 2.65	162.70	◇ -.09	161.7
				▲ .00	162.7
				▼ .11	162.1
				▲ .23	161.6

Configuration	Sound power level, db	Configuration	Sound power level, db
Standard	169.3	Standard	169.30
12-Lobe nozzle	166.3	12-Lobe nozzle	166.30

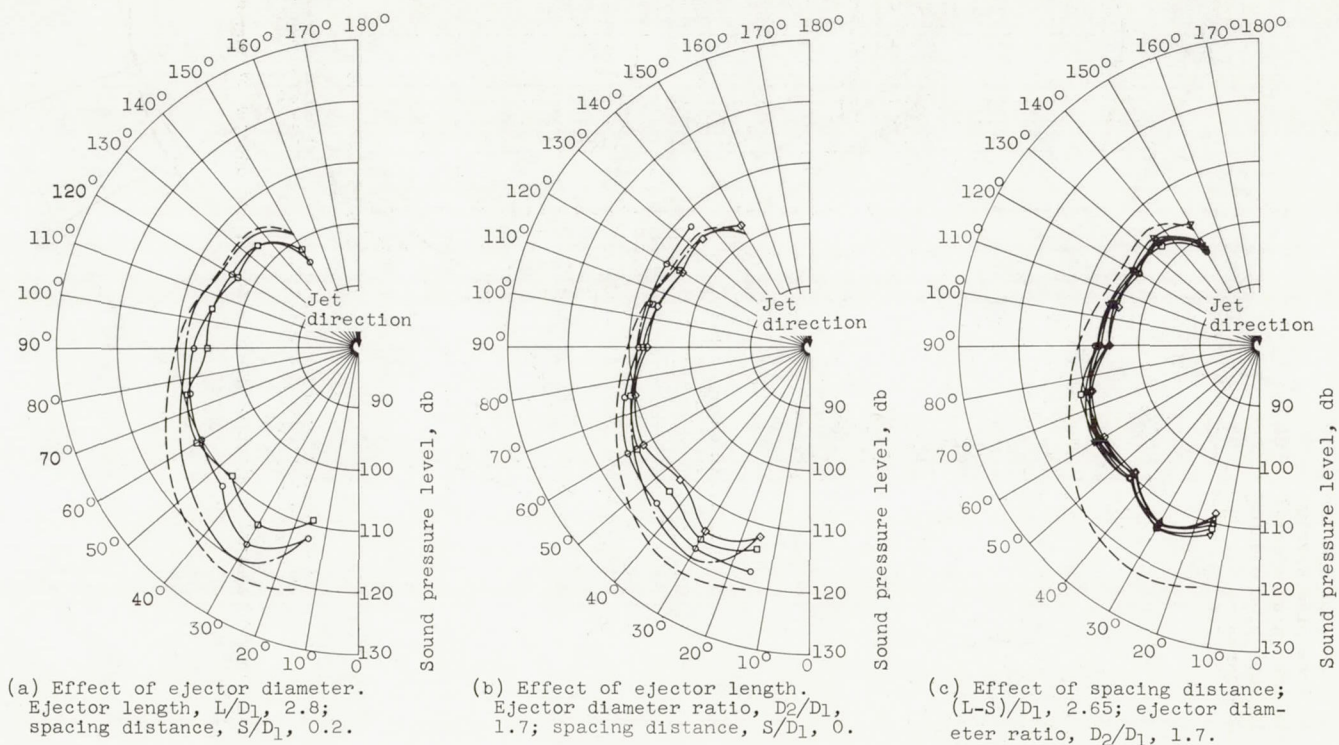


Figure 7. - Effect of various ejector parameters on noise generation. Engine A with 12-lobe nozzle. Velocity, 1700 feet per second.

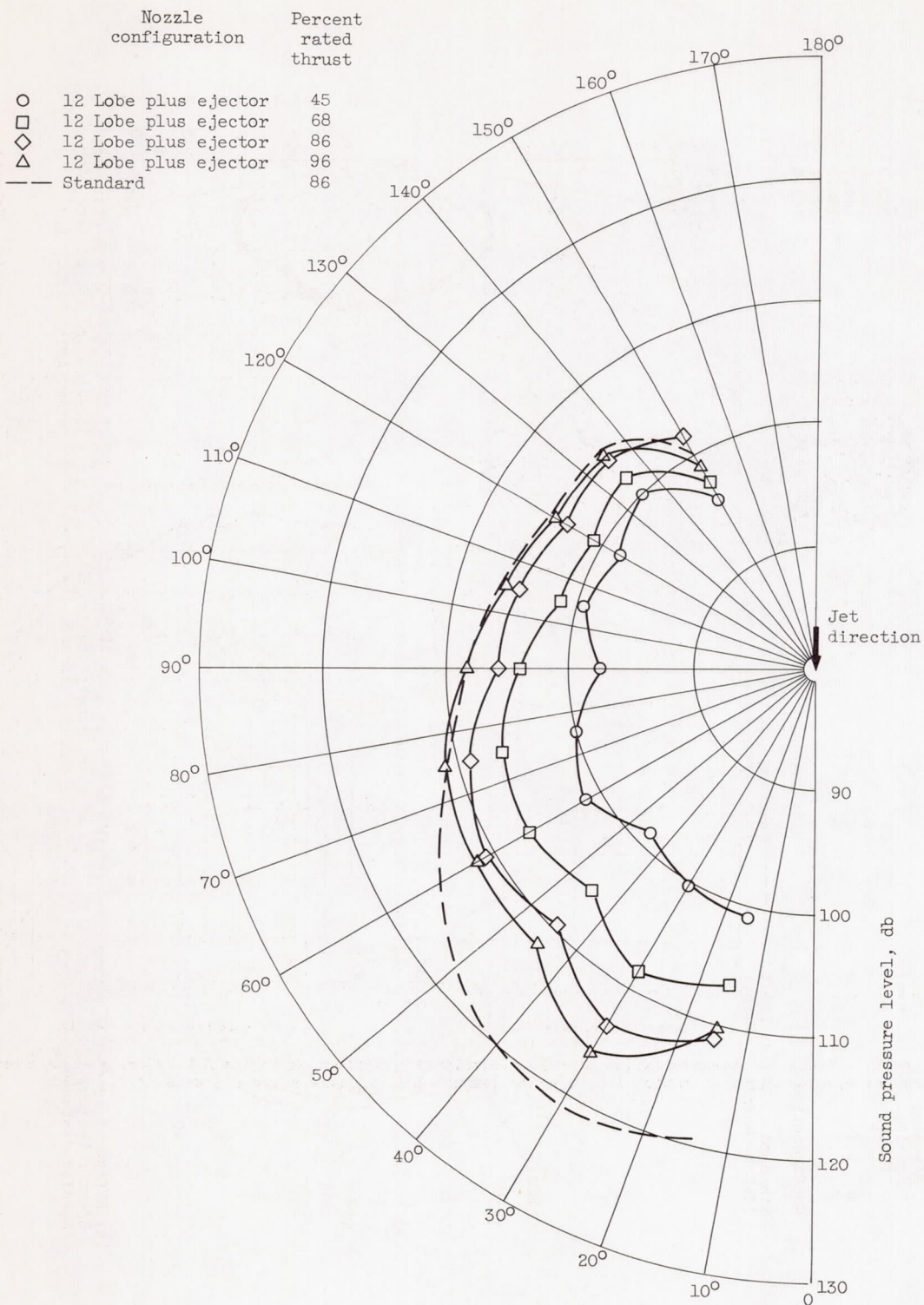


Figure 8. - Effect of engine thrust on noise generation of engine A. Ejector diameter ratio,  $D_2/D_1$ , 1.7; ejector length,  $L/D_1$ , 2.8; spacing distance,  $S/D_1$ , 0.

CZ-4 back 4853

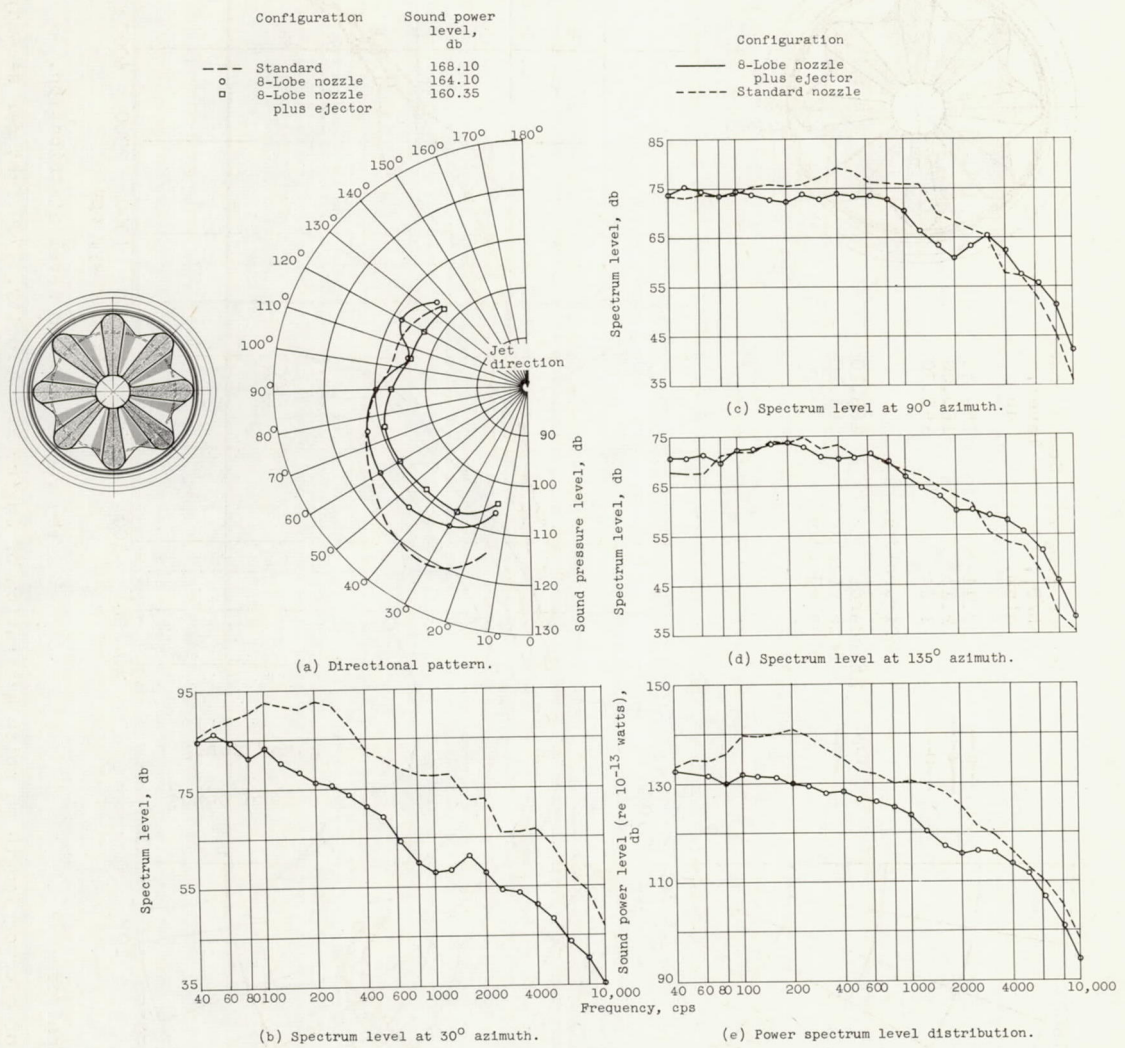


Figure 9. - Acoustic characteristics of 8-lobe nozzle with ejector on engine B. Velocity, 1700 feet per second; ejector diameter ratio, 1.6; ejector length,  $L/D_1$ , 2.4; spacing distance,  $S/D_1$ , 0.10.

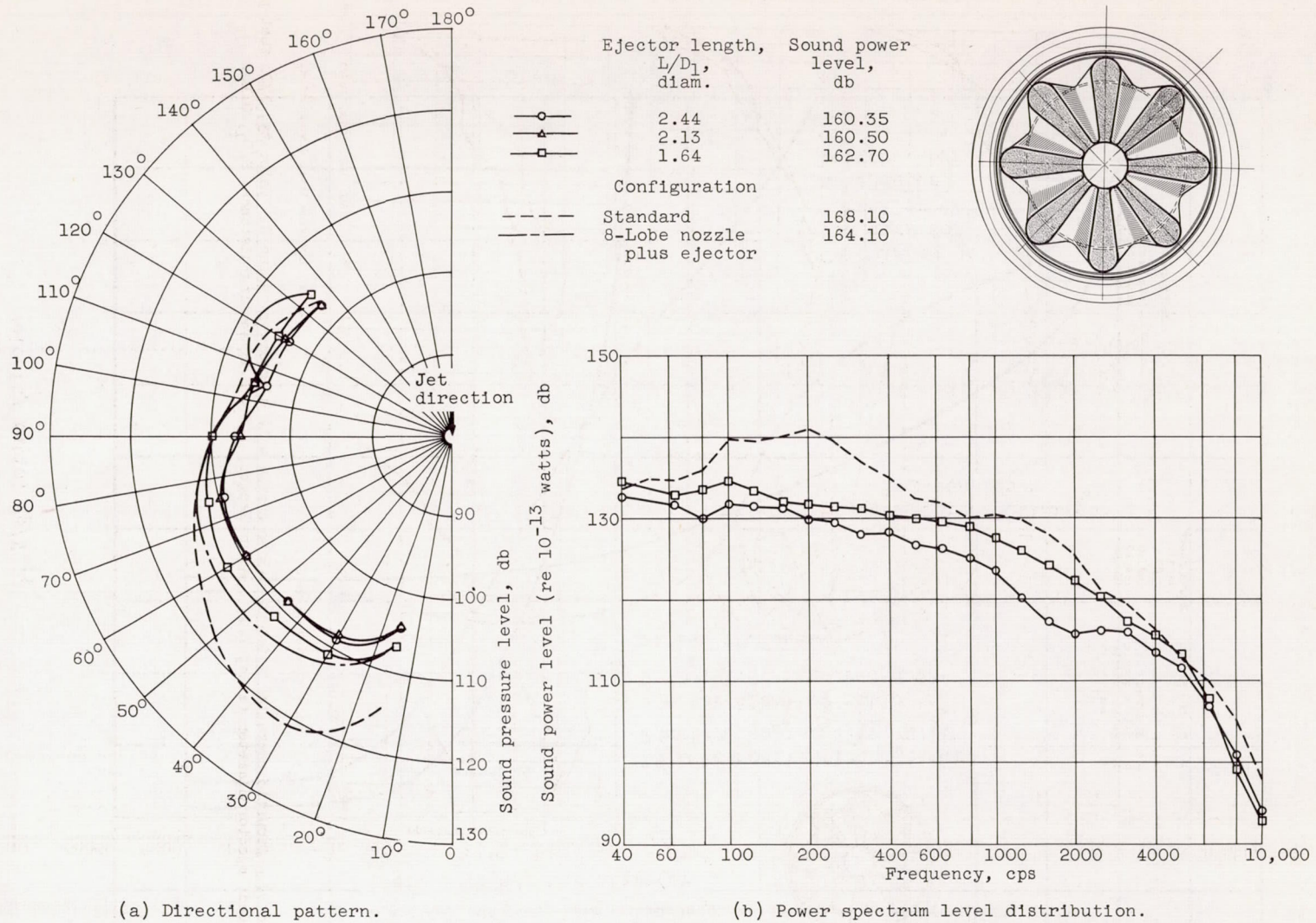


Figure 10. - Effect of ejector length on noise generation of engine B. Velocity, 1700 feet per second; ejector diameter ratio,  $D_2/D_1$ , 1.6; spacing distance,  $S/D_1$ , 0.10.

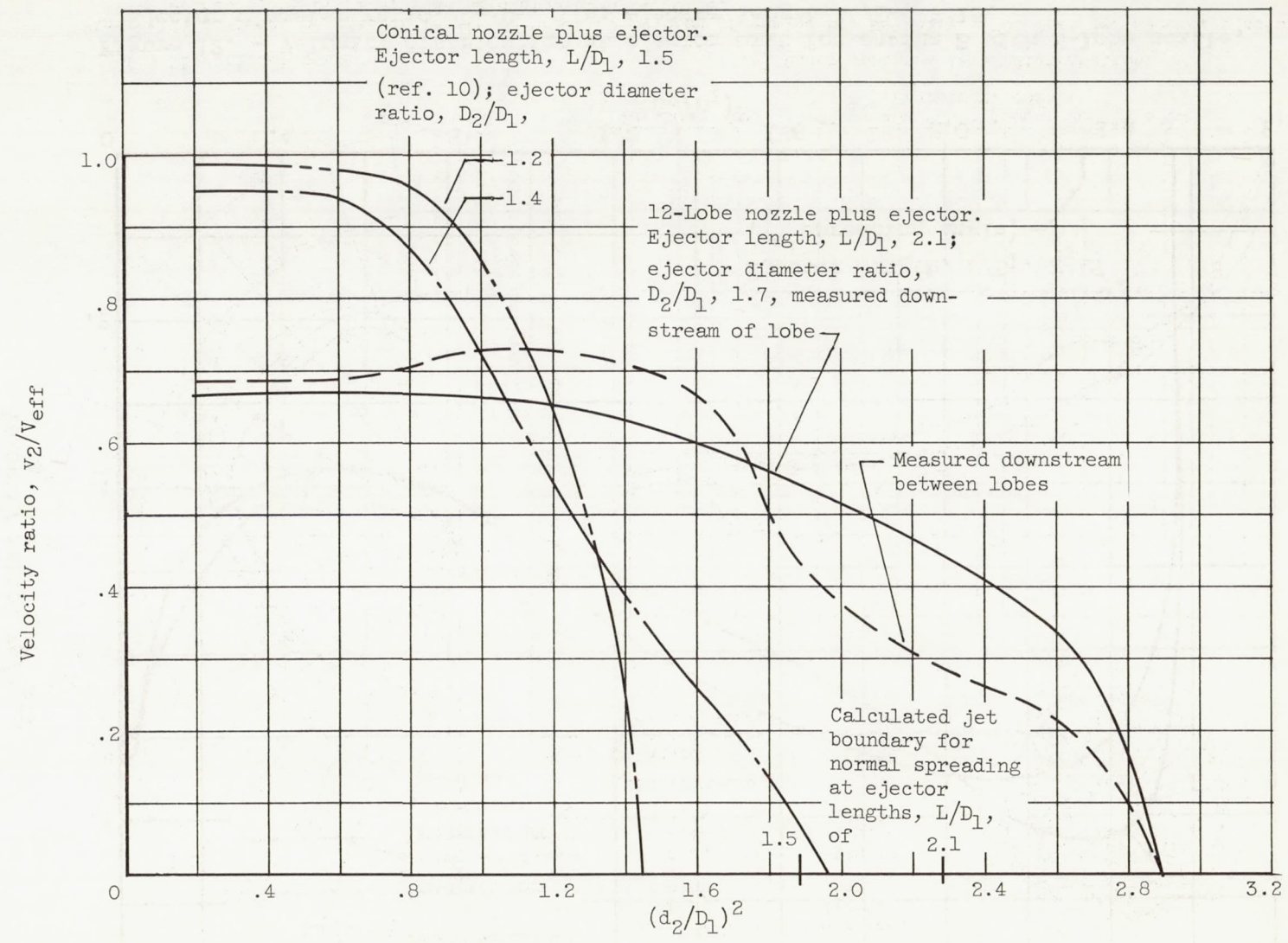


Figure 11. - Velocity distributions at ejector exits.



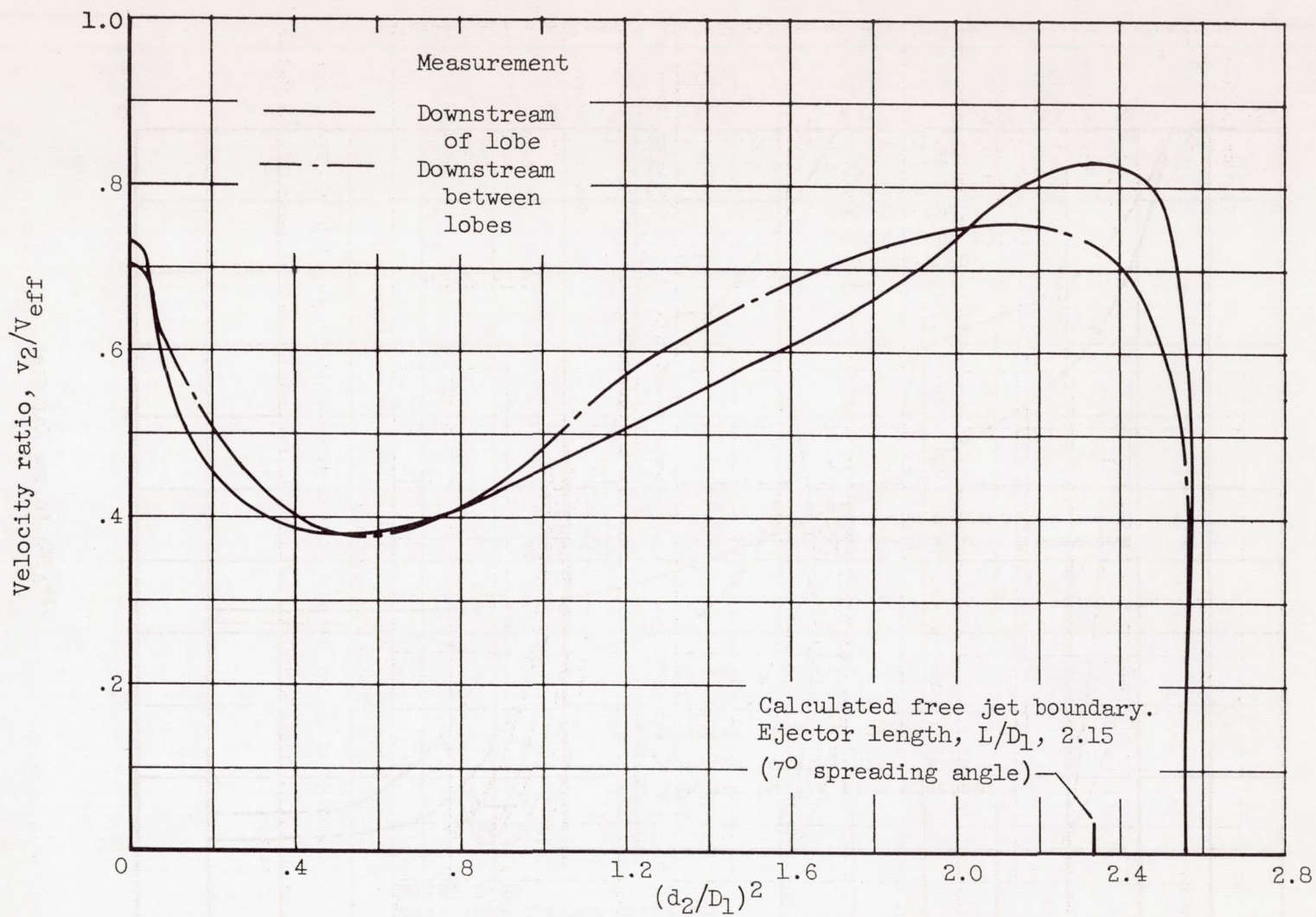


Figure 12. - Velocity distribution at ejector exit for engine B with 8-lobe nozzle. Ejector diameter ratio,  $D_2/D_1$ , 1.6; ejector length,  $L/D_1$ , 2.15.

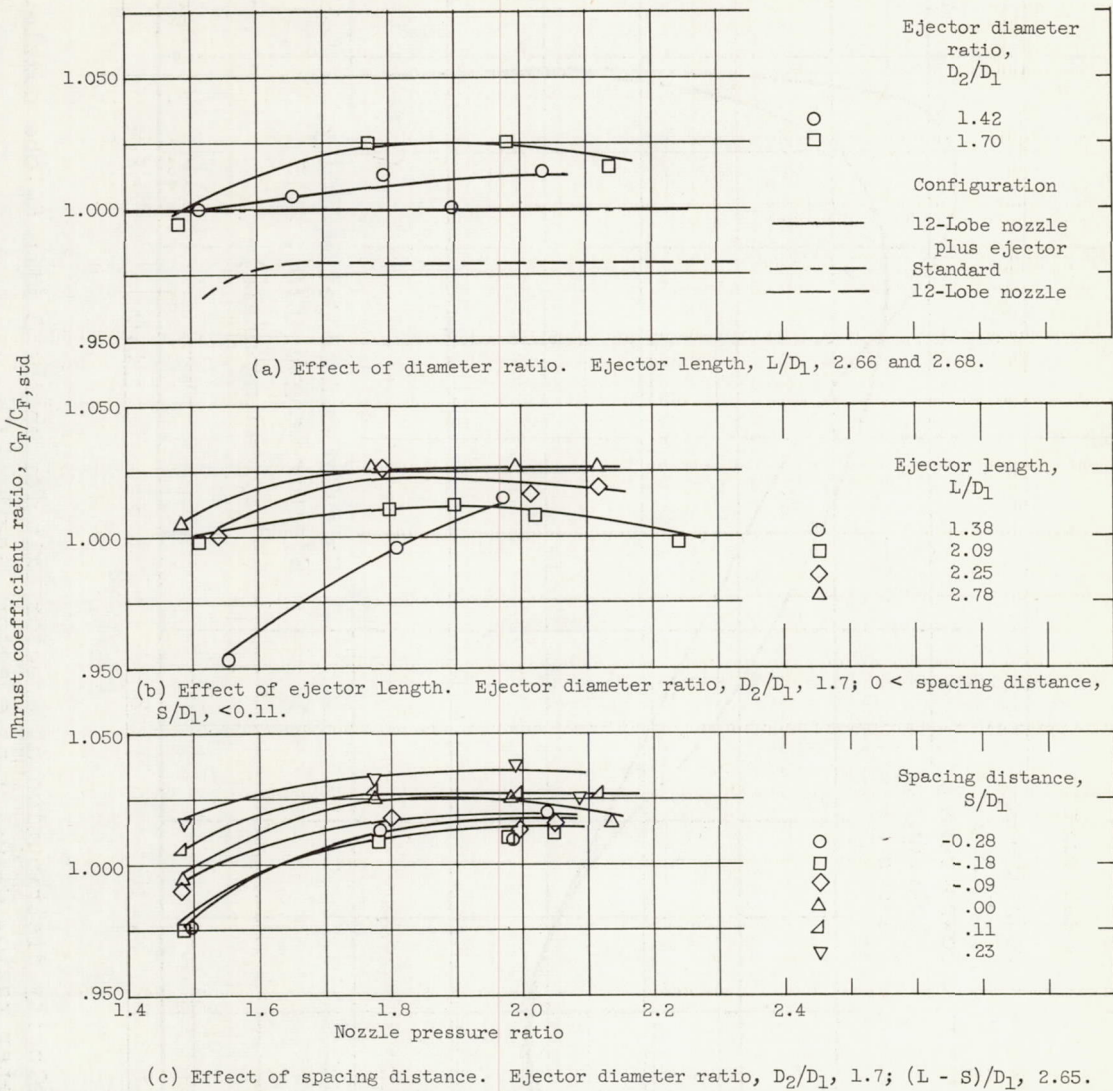


Figure 13. - Thrust coefficient ratio as function of various ejector parameters for 12-lobe nozzle.

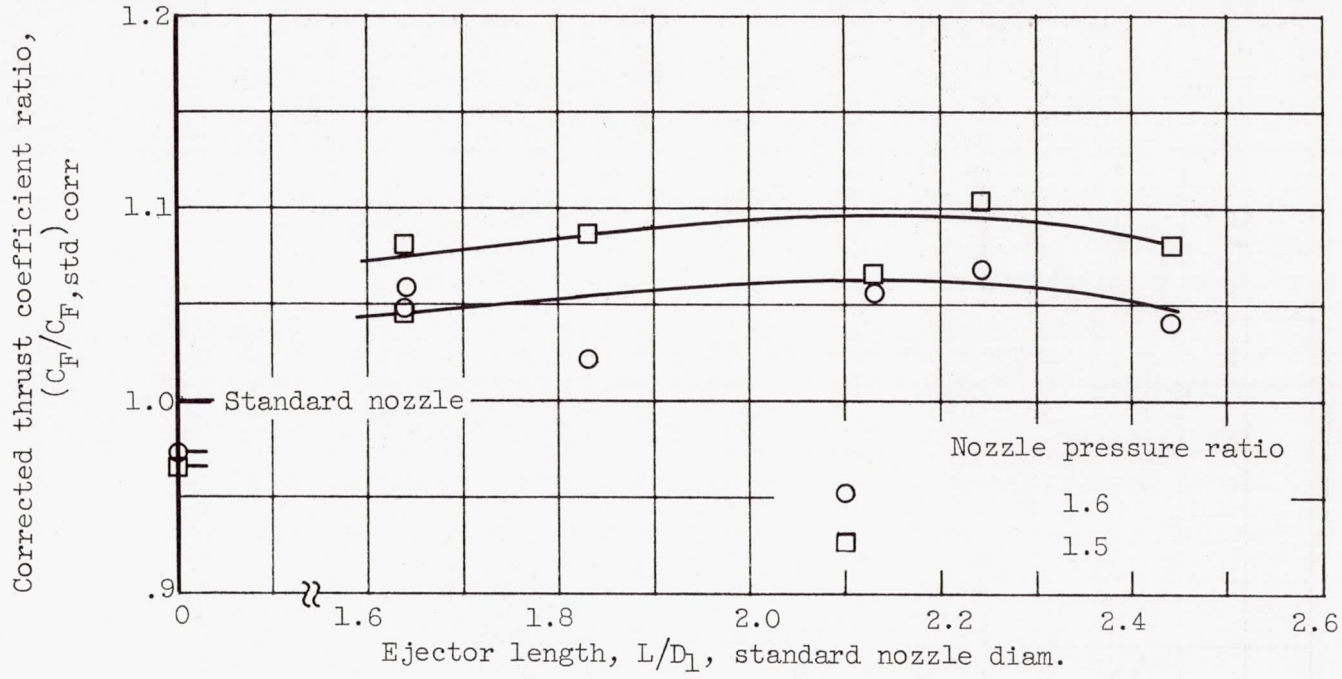


Figure 14. - Effect of ejector length on engine thrust for engine B with 8-lobe nozzle.

